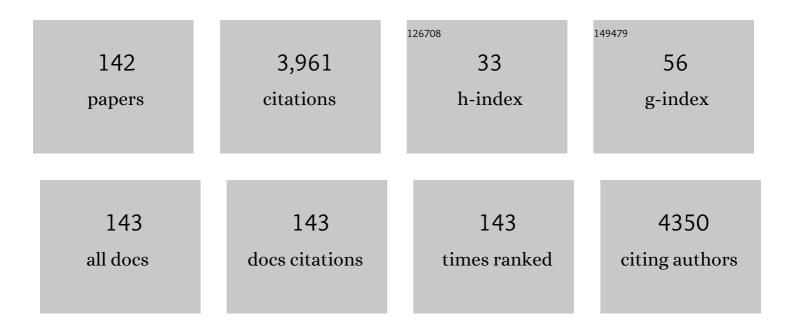
Ping Chen

List of Publications by Year in descending order

Source: https://exaly.com/author-pdf/3056470/publications.pdf Version: 2024-02-01



DINC CHEN

#	Article	IF	CITATIONS
1	Construction of core-shell structured ZnO/C@PPy composite as high-performance dielectric electromagnetic wave absorber. Journal of Magnetism and Magnetic Materials, 2022, 543, 168604.	1.0	6
2	Molecular dynamics simulations of key physical properties and microstructure of epoxy resin cured with different curing agents. Journal of Materials Science, 2022, 57, 1123-1133.	1.7	19
3	Bimetallic nanoarrays embedded in three-dimensional carbon foam as lightweight and efficient microwave absorbers. Carbon, 2022, 191, 486-501.	5.4	30
4	Synthesis of AirRGO@FeCo hollow microspheres with strong microwave absorption properties. Journal of Materials Research, 2022, 37, 1798-1809.	1.2	1
5	Characterization and properties of high-temperature resistant structure adhesive based on novel toughened bismaleimide resins. High Performance Polymers, 2021, 33, 488-496.	0.8	7
6	Synthesis of novel hierarchical CoNi@NC hollow microspheres with enhanced microwave absorption performance. Journal of Materials Science: Materials in Electronics, 2021, 32, 8000-8016.	1.1	12
7	Well-Dispersed Ni Nanoparticles Loaded on Uniform Hollow N-Doped Carbon Spheres for Outstanding Microwave Absorption Performance at a Low Filler Loading. Journal of Electronic Materials, 2021, 50, 4866-4879.	1.0	4
8	Directional Control of the Mechanical Properties of a Resin-Cross-Linking System: A Molecular Dynamics Study. Industrial & Engineering Chemistry Research, 2021, 60, 11621-11626.	1.8	3
9	Constructing and optimizing hollow bird-nest-patterned C@Fe3O4 composites as high-performance microwave absorbers. Journal of Magnetism and Magnetic Materials, 2021, 532, 167990.	1.0	30
10	A review of the bioelectrochemical system as an emerging versatile technology for reduction of antibiotic resistance genes. Environment International, 2021, 156, 106689.	4.8	36
11	Three dimensional flower like ZnFe2O4 ferrite loaded graphene: Enhancing microwave absorption performance by constructing microcircuits. Journal of Alloys and Compounds, 2021, 889, 161734.	2.8	40
12	A modified graphitic carbon nitride (MCN)/Fe ₃ O ₄ composite as a super electromagnetic wave absorber. Journal of Materials Chemistry A, 2021, 9, 23643-23650.	5.2	9
13	Dualâ€system tract pattern: Significance for foreland basin reservoir prediction (Jurassic, Central) Tj ETQq1 1 0.	784314 rg 0.6	gBT_/Overlock
14	The Lower Yangtze area: A next shale gas block for China? Preliminary potential assessment from some geology and organic geochemistry information. Geological Journal, 2020, 55, 3157-3178.	0.6	2
15	Preparation and shape memory behavior of novel heat-resistance epoxy networks containing phthalide cardo structure. Polymer Testing, 2020, 81, 106167.	2.3	4
16	New Chain-Extended Bismaleimides with Aryl-Ether-Imide and Phthalide Cardo Skeleton (II): Creep, Stress Relaxation, Shape Memory and Self-Repairing Properties. Macromolecular Research, 2020, 28, 494-500.	1.0	5
17	Magnetic Dodecahedral CoC-Decorated Reduced Graphene Oxide as Excellent Electromagnetic Wave Absorber. Journal of Electronic Materials, 2020, 49, 1204-1214.	1.0	23
18	Synthesis of reduced graphene oxides with magnetic Co nanocrystals coating for electromagnetic absorption properties. Journal of Materials Science: Materials in Electronics, 2020, 31, 22616-22628.	1.1	3

#	Article	IF	CITATIONS
19	Neutrophil-to-lymphocyte ratio as an independent inflammatory indicator of poor prognosis in IgA nephropathy. International Immunopharmacology, 2020, 87, 106811.	1.7	15
20	Grey Rutile TiO2 with Long-Term Photocatalytic Activity Synthesized Via Two-Step Calcination. Nanomaterials, 2020, 10, 920.	1.9	11
21	Preparation and microwave absorption properties of Ni/rGO/EP composite foam. Journal of Materials Research, 2020, 35, 2106-2114.	1.2	5
22	Environmentally Friendly Synthesis of Velutipes-Shaped Ni@CNTs Composites as Efficient Thin Microwave Absorbers. Journal of Electronic Materials, 2020, 49, 5368-5378.	1.0	5
23	Improving the dynamical seasonal prediction of western Pacific warm pool sea surface temperatures using a physical–empirical model. International Journal of Climatology, 2020, 40, 4657-4675.	1.5	5
24	Improvement of the interfacial properties of PBO/Epoxy composites by online continuous plasma grafting with polyurethane. Progress in Organic Coatings, 2020, 143, 105610.	1.9	8
25	Influence of DBD-grafted multi-carboxyl polyurethane on interfacial properties of PBO fibre-reinforced BMI resin composites. Applied Surface Science, 2020, 512, 145662.	3.1	15
26	Roundâ€ŧhe lock Photocatalytic Hydrogen Production with High Efficiency by a Longâ€Afterglow Material. Angewandte Chemie, 2019, 131, 1354-1358.	1.6	8
27	Properties of novel bismaleimide resins and thermal ageing effects on the ILSS performance of their carbon fibre–bismaleimide composites. Polymer Composites, 2019, 40, E1283.	2.3	10
28	Graphene anchored with super-tiny Ni nanoparticles for high performance electromagnetic absorption applications. Journal of Materials Science: Materials in Electronics, 2019, 30, 14480-14489.	1.1	5
29	Solvothermal synthesis of porous superparamagnetic RGO@Fe3O4 nanocomposites for microwave absorption. Journal of Materials Science: Materials in Electronics, 2019, 30, 17106-17118.	1.1	8
30	Hydrogenation of Dicyclopentadiene Resin and Its Monomer over High Efficient CuNi Alloy Catalysts. ChemistrySelect, 2019, 4, 6035-6042.	0.7	13
31	In situ deposition of α-Co nanoparticles on three-dimensional nitrogen-doped porous graphene foams as microwave absorbers. Journal of Materials Science: Materials in Electronics, 2019, 30, 13412-13424.	1.1	5
32	A novel multifunctional glycidylamine epoxy resin containing phthalide cardo structure: Synthesis, curing kinetics and dynamic mechanical analysis. Polymer Testing, 2019, 77, 105917.	2.3	19
33	Reduced Graphene Oxide-Wrapped Super Dense Fe3O4 Nanoparticles with Enhanced Electromagnetic Wave Absorption Properties. Nanomaterials, 2019, 9, 845.	1.9	11
34	MoS2 Nanosheets Assembled on Three-Way Nitrogen-Doped Carbon Tubes for Photocatalytic Water Splitting. Frontiers in Chemistry, 2019, 7, 325.	1.8	9
35	Two-step synthesis of self-assembled 3D graphene/shuttle-shaped zinc oxide (ZnO) nanocomposites for high-performance microwave absorption. Journal of Alloys and Compounds, 2019, 797, 1310-1319.	2.8	48
36	Synthesis of magnetic graphene aerogels for microwave absorption by in-situ pyrolysis. Carbon, 2019, 146, 301-312.	5.4	116

Ping Chen

#	Article	IF	CITATIONS
37	<i>In situ</i> growth and pyrolysis synthesis of super-hydrophobic graphene aerogels embedded with ultrafine β-Co nanocrystals for microwave absorption. Journal of Materials Chemistry C, 2019, 7, 3869-3880.	2.7	42
38	Superior corrosion-resistant 3D porous magnetic graphene foam-ferrite nanocomposite with tunable electromagnetic wave absorption properties. Journal of Magnetism and Magnetic Materials, 2019, 469, 428-436.	1.0	48
39	3D nitrogen-doped porous magnetic graphene foam-supported Ni nanocomposites with superior microwave absorption properties. Journal of Alloys and Compounds, 2019, 782, 600-610.	2.8	33
40	Microwave absorbing and mechanical properties of carbon fiber/bismaleimide composites imbedded with Fe@C/PEK-C nano-membranes. Journal of Materials Science: Materials in Electronics, 2019, 30, 308-315.	1,1	5
41	Investigation of the curing mechanism and properties of bismaleimideâ€ŧriazine resins containing phenolphthalein and cyano group. Journal of Applied Polymer Science, 2019, 136, 47420.	1.3	7
42	Roundâ€ŧhe lock Photocatalytic Hydrogen Production with High Efficiency by a Longâ€Afterglow Material. Angewandte Chemie - International Edition, 2019, 58, 1340-1344.	7.2	67
43	Synthesis and properties of bismaleimide resins containing phthalide cardo and cyano groups. High Performance Polymers, 2019, 31, 462-471.	0.8	6
44	Thermal, mechanical properties and shape memory performance of a novel phthalide-containing epoxy resins. Polymer, 2018, 140, 326-333.	1.8	28
45	Mechanical performance of 3D-printing plastic honeycomb sandwich structure. International Journal of Precision Engineering and Manufacturing - Green Technology, 2018, 5, 47-54.	2.7	29
46	Effect of exopolysaccharides-producing strain on oxidation stability of DHA micro algae oil microcapsules. Food Bioscience, 2018, 23, 60-66.	2.0	7
47	The thermal decomposition behavior and kinetics of epoxy resins cured with a novel phthalide-containing aromatic diamine. Polymer Testing, 2018, 68, 46-52.	2.3	30
48	Photoluminescent F-doped carbon dots prepared by ring-opening reaction for gene delivery and cell imaging. RSC Advances, 2018, 8, 6053-6062.	1.7	45
49	New chain-extended bismaleimides with aryl-ether-imide and phthalide cardo skeleton (I): Synthesis, characterization and properties. Reactive and Functional Polymers, 2018, 129, 29-37.	2.0	11
50	Cure mechanism of novel bismaleimide resins based on fluorene cardo moiety and their thermal properties. Journal of Macromolecular Science - Pure and Applied Chemistry, 2018, 55, 213-221.	1.2	3
51	Improvement of aramid fiber III reinforced bismaleimide composite interfacial adhesion by oxygen plasma treatment. Composite Interfaces, 2018, 25, 771-783.	1.3	22
52	Novel Bismaleimide Resins Modified by Allyl Compound Containing Liquid Crystalline Structure. Advances in Polymer Technology, 2018, 37, 281-289.	0.8	12
53	Bismaleimide-diamine copolymers containing phthalide cardo structure and their modified BMI resins. High Performance Polymers, 2018, 30, 527-538.	0.8	6
54	3D graphene-Ni microspheres with excellent microwave absorption and corrosion resistance properties. Journal of Materials Science: Materials in Electronics, 2018, 29, 2421-2433.	1.1	42

#	Article	IF	CITATIONS
55	Effect of waxy rice starch on textural and microstructural properties of microwaveâ€puffed cheese chips. International Journal of Dairy Technology, 2018, 71, 501-511.	1.3	10
56	The effect of phthalide cardo structure on the shape memory performance of high-temperature resistant epoxy resins. Materials Research Express, 2018, 5, 115702.	0.8	6
57	Synthesis of popcorn-like α-Fe2O3/3D graphene sponge composites for excellent microwave absorption properties by a facile method. Journal of Materials Science: Materials in Electronics, 2018, 29, 19443-19453.	1.1	19
58	NMR study on the coordination of diperoxovanadium(V) complexes with 2-hydroxymethyl pyridine derivatives. Journal of Coordination Chemistry, 2018, 71, 3117-3126.	0.8	2
59	Alkynyl-functionalized benzoxazine containing phthalide side group: Synthesis, characterization and curing mechanism. Polymer Testing, 2018, 72, 232-237.	2.3	18
60	Enhanced microwave absorption properties of electrospun PEK nanofibers loaded with Fe ₃ O ₄ /CNTs hybrid nanoparticles. Polymer Engineering and Science, 2017, 57, 1186-1192.	1.5	6
61	Wettability assessment of plasma-treated PBO fibers based on thermogravimetric analysis. International Journal of Adhesion and Adhesives, 2017, 74, 123-130.	1.4	14
62	Synthesis and electromagnetic absorption properties of Fe3O4@C nanofibers/bismaleimide nanocomposites. Journal of Materials Science: Materials in Electronics, 2017, 28, 2769-2774.	1.1	13
63	Synthesis and electromagnetic wave absorption properties of matrimony vine-like iron oxide/reduced graphene oxide prepared by a facile method. Journal of Alloys and Compounds, 2017, 719, 296-307.	2.8	46
64	Interface characteristic of aramid fiber reinforced poly(phthalazinone ether sulfone ketone) composite. Surface and Interface Analysis, 2017, 49, 788-793.	0.8	15
65	Self-assembly of ternary hollow microspheres with strong wideband microwave absorption and controllable microwave absorption properties. Scientific Reports, 2017, 7, 8388.	1.6	32
66	Aging behavior of dielectric barrier dischargeâ€modified Twaron fibers in different storage environments. Surface and Interface Analysis, 2017, 49, 419-426.	0.8	4
67	Effects of oxygen plasma treatment on domestic aramid fiber III reinforced bismaleimide composite interfacial properties. IOP Conference Series: Materials Science and Engineering, 2017, 274, 012104.	0.3	1
68	Tunable reflecting terahertz filter based on chirped metamaterial structure. Scientific Reports, 2016, 6, 38732.	1.6	37
69	Strong confinement of THz pulse by femtosecond laser filamentation. , 2016, , .		0
70	3D and ternary rGO/MCNTs/Fe3O4 composite hydrogels: Synthesis, characterization and their electromagnetic wave absorption properties. Journal of Alloys and Compounds, 2016, 665, 381-387.	2.8	145
71	Surface adhesive properties of continuous PBO fiber after air-plasma-grafting-epoxy treatment. Journal of Central South University, 2016, 23, 2165-2172.	1.2	5
72	Air@rGOâ,¬Fe ₃ O ₄ microspheres with spongy shells: self-assembly and microwave absorption performance. Journal of Materials Chemistry C, 2016, 4, 10518-10528.	2.7	77

#	Article	IF	CITATIONS
73	The effect of atmosphericâ€pressure air plasma discharge power on adhesive properties of aramid fibers. Polymer Composites, 2016, 37, 620-626.	2.3	20
74	lsothermal curing kinetics and mechanism of DGEBA epoxy resin with phthalide-containing aromatic diamine. Thermochimica Acta, 2016, 623, 15-21.	1.2	41
75	Synthesis of novel bismaleimide monomers based on fluorene cardo moiety and ester bond: Characterization and thermal properties. Journal of Macromolecular Science - Pure and Applied Chemistry, 2016, 53, 88-95.	1.2	8
76	Preparation and properties of bismaleimide resins based on novel bismaleimide monomer containing fluorene cardo structure. High Performance Polymers, 2016, 28, 215-224.	0.8	9
77	Stress Distribution on Composite Honeycomb Sandwich Structure Suffered from Bending Load. Procedia Engineering, 2015, 99, 405-412.	1.2	39
78	Preparation and properties of modified bismaleimide resins by novel bismaleimide containing 1,3,4â€oxadiazole. Polymers for Advanced Technologies, 2015, 26, 266-276.	1.6	24
79	Comparison of effects on PBO fiber by air and oxygen dielectric barrier discharge plasma. Vacuum, 2015, 121, 152-158.	1.6	12
80	Degradation of plasma-treated poly(p-phenylene benzobisoxazole) fiber and its adhesion with bismaleimide resin. RSC Advances, 2014, 4, 3893-3899.	1.7	5
81	Synthesis and properties of 1,3,4-oxadiazole-containing bismaleimides with asymmetric structure and the copolymerized systems thereof with 4,4′-bismaleimidodiphenylmethane. RSC Advances, 2014, 4, 4646-4655.	1.7	22
82	Modification of carbon fiber by air plasma and its adhesion with BMI resin. RSC Advances, 2014, 4, 26881.	1.7	50
83	The curing kinetics and thermal properties of epoxy resins cured by aromatic diamine with hetero-cyclic side chain structure. Thermochimica Acta, 2014, 595, 22-27.	1.2	35
84	Synthesis, characterization, and curing kinetics of novel bismaleimide monomers containing fluorene cardo group and aryl ether linkage. Designed Monomers and Polymers, 2014, 17, 637-646.	0.7	21
85	Effects of electron irradiation in space environment on thermal and mechanical properties of carbon fiber/bismaleimide composite. Nuclear Instruments & Methods in Physics Research B, 2014, 336, 158-162.	0.6	21
86	Improved mechanical performance of PBO fiber-reinforced bismaleimide composite using mixed O2/Ar plasma. Applied Surface Science, 2014, 305, 630-637.	3.1	20
87	Effect of thermoplastic coating on interfacial adhesion of oxygen-plasma-pretreated PBO/PPESK composites. Applied Surface Science, 2013, 266, 110-117.	3.1	14
88	Electrochemical performance and thermal property of electrospun PPESK/PVDF/PPESK composite separator for lithium-ion battery. Journal of Applied Electrochemistry, 2013, 43, 711-720.	1.5	41
89	Effects of plasma-induced epoxy coatings on surface properties ofÂTwaron fibers and improved adhesion with PPESK resins. Vacuum, 2013, 97, 1-8.	1.6	14
90	Effects of surface modification by atmospheric oxygen dielectric barrier discharge plasma on PBO fibers and its composites. Applied Surface Science, 2013, 283, 38-45.	3.1	20

#	Article	IF	CITATIONS
91	Atmospheric air plasma treated PBO fibers: Wettability, adhesion and aging behaviors. Vacuum, 2013, 92, 13-19.	1.6	25
92	Degradation in mechanical and physical properties of carbon fiber/bismaleimide composite subjected to proton irradiation in a space environment. Nuclear Instruments & Methods in Physics Research B, 2013, 298, 42-46.	0.6	16
93	Hydrothermal synthesis of macroscopic nitrogen-doped graphene hydrogels for ultrafast supercapacitor. Nano Energy, 2013, 2, 249-256.	8.2	530
94	Cure mechanism and thermal properties of the phthalide-containing bismaleimide/epoxy system. Thermochimica Acta, 2013, 559, 52-58.	1.2	16
95	The effects of zirconium diboride particles on the ablation performance of carbon–phenolic composites under an oxyacetylene flame. RSC Advances, 2013, 3, 13734.	1.7	29
96	Effect of plasma modification on the mechanical properties of carbon fiber/phenolphthalein polyaryletherketone composites. Polymer Composites, 2013, 34, 368-375.	2.3	37
97	Preparation and properties of modified bismaleimide resins based on phthalideâ€containing monomer. Journal of Applied Polymer Science, 2013, 130, 1084-1091.	1.3	26
98	Photocatalytic activity of MnWO4 powder in highly effective hydrogen generation from H2O and H2O2. International Journal of Materials Research, 2012, 103, 1265-1270.	0.1	2
99	The interfacial adhesion of poly-p-phenylene benzobisoxazole/bismaleimide composites improved by oxygen/argon plasma treatment and surface aging effects. Surface and Coatings Technology, 2012, 207, 221-226.	2.2	11
100	Improvement of PBO fiber surface and PBO/PPESK composite interface properties with air DBD plasma treatment. Surface and Interface Analysis, 2012, 44, 548-553.	0.8	17
101	Wetting and adhesion behavior of armos fibers after dielectric barrier discharge plasma treatment. Journal of Applied Polymer Science, 2012, 125, 433-438.	1.3	8
102	Electrochemical performances and thermal properties of electrospun Poly(phthalazinone ether) Tj ETQq0 0 0 rgB	T /Oyerloc 1.3	k 10 Tf 50 30
103	Improved interfacial adhesion in PBO fiber/bismaleimide composite with oxygen plasma plus aging and humid resistance properties. Materials Science & Engineering A: Structural Materials: Properties, Microstructure and Processing, 2012, 532, 78-83.	2.6	15
104	Surface modification of high performance PBO fibers using radio frequency argon plasma. Surface and Coatings Technology, 2012, 206, 3534-3541.	2.2	32
105	Improvement of the interfacial adhesion between PBO fibers and PPESK matrices using plasmaâ€induced coating. Journal of Applied Polymer Science, 2012, 123, 2945-2951.	1.3	11
106	Effects of argon plasma treatment on the interfacial adhesion of PBO fiber/bismaleimide composite and aging behaviors. Applied Surface Science, 2011, 257, 10239-10245.	3.1	30
107	Effects of air dielectric barrier discharge plasma treatment time on surface properties of PBO fiber. Applied Surface Science, 2011, 258, 513-520.	3.1	23

108Surface wettability of atmospheric dielectric barrier discharge processed Armos fibers. Applied
Surface Science, 2011, 258, 388-393.3.115

#	ARTICLE	IF	CITATIONS
109	Synthesis and Electromagnetic, Microwave Absorbing Properties of Core–Shell Fe ₃ O ₄ –Poly(3, 4-ethylenedioxythiophene) Microspheres. ACS Applied Materials & Interfaces, 2011, 3, 3839-3845.	4.0	265
110	Effects of vacuum thermal cycling on mechanical and physical properties of high performance carbon/bismaleimide composite. Materials Chemistry and Physics, 2011, 130, 1046-1053.	2.0	33
111	Surface molecular degradation of high performance carbon/bismaleimide composites induced by proton irradiation. Nuclear Instruments & Methods in Physics Research B, 2011, 269, 318-323.	0.6	9
112	Synthesis and properties of a novel bismaleimide resin containing 1,3,4â€oxadiazole moiety and the blend systems thereof with epoxy resin. Polymer Engineering and Science, 2011, 51, 1599-1606.	1.5	21
113	Surface analysis of high performance carbon/bismaleimide composites exposed to electron irradiation. Surface and Interface Analysis, 2011, 43, 1610-1615.	0.8	9
114	Preparation and properties of high performance phthalideâ€containing bismaleimide modified epoxy matrices. Journal of Applied Polymer Science, 2011, 121, 3122-3130.	1.3	22
115	Influence of cyanate content on the morphology and properties of epoxy resins with phenolphthalein poly(ether ketone). Journal of Applied Polymer Science, 2011, 121, 598-603.	1.3	13
116	Surface modification of armos fibers with oxygen plasma treatment for improving interfacial adhesion with poly(phthalazinone ether sulfone ketone) resin. Journal of Applied Polymer Science, 2011, 121, 2804-2811.	1.3	10
117	Surface treatment of aramid fiber by air dielectric barrier discharge plasma at atmospheric pressure. Applied Surface Science, 2011, 257, 4165-4170.	3.1	106
118	Improvement and mechanism of interfacial adhesion in PBO fiber/bismaleimide composite by oxygen plasma treatment. Applied Surface Science, 2011, 257, 6935-6940.	3.1	44
119	Cure kinetics and thermal properties of novel bismaleimide containing phthalide cardo structure. Thermochimica Acta, 2011, 514, 44-50.	1.2	22
120	Effects of Twaron fiber surface treatment by air dielectric barrier discharge plasma on the interfacial adhesion in fiber reinforced composites. Surface and Coatings Technology, 2010, 204, 3668-3675.	2.2	57
121	A study of the effect of oxygen plasma treatment on the interfacial properties of carbon fiber/epoxy composites. Journal of Applied Polymer Science, 2010, 118, 1606-1614.	1.3	46
122	Influence of collecting velocity on fiber orientation, morphology and tensile properties of electrospun PPESK fabrics. Journal of Applied Polymer Science, 2010, 118, 2236-2243.	1.3	1
123	Synthesis and properties of chainâ€extended bismaleimide resins containing phthalide cardo structure. Polymer International, 2010, 59, 1665-1672.	1.6	46
124	Thermal Stress Distribution in CF/EP Composite in Low Earth Orbit. Journal of Composite Materials, 2010, 44, 1729-1738.	1.2	8
125	Reaction kinetics and thermal properties of cyanate esterâ€cured epoxy resin with phenolphthalein poly(ether ketone). Journal of Applied Polymer Science, 2009, 111, 2590-2596.	1.3	23
126	Influence of oxygen plasma treatment on interfacial properties of poly(<i>p</i> â€phenylene) Tj ETQq0 0 0 rgBT	/Overlock] 1.3	10 Tf 50 67 T 12

Applied Polymer Science, 2009, 113, 71-77.

Ping Chen

#	Article	IF	CITATIONS
127	Improvement of interfacial adhesion for plasmaâ€treated aramid fiberâ€reinforced poly(phthalazinone) Tj ETQq1 41, 38-43.	1 0.78431 0.8	.4 rgBT /Ove 29
128	Aging behavior of PBO fibers and PBOâ€fiberâ€reinforced PPESK composite after oxygen plasma treatment. Surface and Interface Analysis, 2009, 41, 187-192.	0.8	18
129	Influence of aging behavior of Armos fiber after oxygen plasma treatment on its composite interfacial properties. Surface and Coatings Technology, 2009, 203, 3722-3727.	2.2	17
130	Surface analysis of oxygen plasma treated poly(p-phenylene benzobisoxazole) fibers. Applied Surface Science, 2008, 254, 5776-5780.	3.1	34
131	The analysis of Armos fibers reinforced poly(phthalazinone ether sulfone ketone) composite surfaces after oxygen plasma treatment. Surface and Coatings Technology, 2008, 202, 4986-4991.	2.2	12
132	Two-photon spectroscopic behaviors and photodynamic effect on the BEL-7402 cancer cells of the new chlorophyll photosensitizer. Science in China Series B: Chemistry, 2008, 51, 529-538.	0.8	8
133	Thermal Residual Stress Distribution in Carbon Fiber/Novel Thermal Plastic Composite. Applied Composite Materials, 2008, 15, 157-169.	1.3	21
134	Surface characteristic of poly(<i>p</i> â€phenylene terephthalamide) fibers with oxygen plasma treatment. Surface and Interface Analysis, 2008, 40, 1299-1303.	0.8	36
135	Effects of oxygen plasma treatment power on surface properties of poly(p-phenylene benzobisoxazole) fibers. Applied Surface Science, 2008, 255, 3153-3158.	3.1	41
136	Use of Near-Infrared Spectroscopy for On-Line Monitoring the Quality of Prepreg Cloth. Advanced Composites Letters, 2008, 17, 096369350801700.	1.3	5
137	Nir Spectroscopy: A Useful Tool for Quality Control of Glass/Phenolic Prepreg Manufacture. Polymers and Polymer Composites, 2008, 16, 55-62.	1.0	3
138	Computer Simulation of Thermal Residual Stress of Carbon Fibre/Ppesk Composite. Advanced Composites Letters, 2007, 16, 096369350701600.	1.3	3
139	Interfacial adhesion of plasma-treated carbon fiber/poly(phthalazinone ether sulfone ketone) composite. Journal of Applied Polymer Science, 2007, 106, 1733-1741.	1.3	68
140	Computer simulation of electrospinning. Part I. Effect of solvent in electrospinning. Polymer, 2006, 47, 915-921.	1.8	66
141	Influence of fiber wettability on the interfacial adhesion of continuous fiber-reinforced PPESK composite. Journal of Applied Polymer Science, 2006, 102, 2544-2551.	1.3	89
142	Influence of Oxygen Plasma Treatment on Surface Properties of Armos Fiber. Key Engineering Materials, 0, 373-374, 430-433.	0.4	2